Communications in Physics, Vol. 33, No. 2 (2023), pp. 157-168
DOI: https://doi.org/10.15625/0868-3166/17517

Investigation of the radiative decay $b \to s\gamma$ in the 3-4-1-1 model

Nguyen Tuan Duy† **and Do Thi Huong**

Institute of Physics, Vietnam Academy of Science and Technology
10 Dao Tan, Ba Dinh, Hanoi 11108, Vietnam

E-mail: †ntduy@iop.vast.vn

Received 17 September 2022
Accepted for publication 20 October 2022
Published 21 April 2023

Abstract. *We investigate the branching ratio of the radiative decay $b \to s\gamma$ in the 3-4-1-1 model with arbitrary charge parameters p, q. We show that the new Higgs bosons, $\mathscr{H}_1^{\pm}$, and the new gauge bosons $W_{13,14}^{\pm q,p}, W_{23,24}^{\pm(q+1),(p+1)}, Z_{2,3}$ contribute to this decay. Of these sources, the main contribution comes from the interaction of the singly-charged Higgs boson. If the spontaneous breaking of the gauge group symmetry down to the electroweak group is around a few TeVs, the predictions for the branching ratio $Br(b \to s\gamma)$ and meson mixing are consistent with experimental constraints.*

Keywords: radiative corrections; models beyond the standard model; dark matter.

Classification numbers: 95.35.+d;12.60.-i;12.15.Lk.

1. Introduction

Although the Standard Model (SM) is the most successful in explaining the observed elementary particle phenomena, it is incomplete due to the experimental evidence of neutrino oscillation showing the existence of nonzero but tiny and mixing neutrino masses [1, 2]. The SM cannot explain the cosmological phenomena such as inflation, baryon asymmetry, and dark matter (DM) [3]. The SM describes only about 5% visible matter of the universe, whereas the remaining of $\simeq 25\%$ DM and $\simeq 70\%$ dark energy cannot be explained. Most previous theories [4–14] have suggested that DM is composed of a kind of a single particle - the lightest particle that is odd under the discrete symmetry. However, the components of DM are still unclear. There is no argument that DM has only one component, and thus, a multicomponent model can arise naturally. Moreover, the phenomenology and theory, which have been studied in multicomponent models [15–23], have yielded interesting consequences for galaxy structure [24,25]. The predictions of multicomponent DM models have been matched to the multiple gamma-ray lines, boosted DM signals, and DM self-interactions [26–30]. Among the extended gauge symmetry models, the model with a higher weak isospin symmetry $SU(P)_L$ combined with two factors, $U(1)_X \times U(1)_N$, which determine the electric charge and noncommutative $B-L$ charge, not only provides natural solutions for multicomponent DM but also solves the current issues [20,21]. In the SM, the $[SU(2)_L]^3$ anomaly vanishes for every representation. If the $SU(2)_L$ symmetry of weak isospin is extended to $SU(P)_L$ for $P = 3,4,5,...$, the $[SU(P)_L]^3$ anomaly cancellation requests that the number of fermion P-plets equals the number of fermion anti-P-plets. Depending on the arrangement of the particle content, the kind of model leads to the existence of flavor changing neutral currents (FCNCs) at the tree level for quark or lepton sectors. In this work, we investigate the minimal multicomponent DM (MMDM) model , which is based on the $SU(3)_C \otimes SU(4)_L \otimes U(1)_X \otimes U(1)_N$ gauge groups, the so-called 3-4-1-1 model [20,21]. Because of the different arrangement of quark generations, the model predicted the existence of the FCNC at the tree level in the quark sector. This causes the model to face many constraints from flavor physics, such as the oscillations of the meson system [31], the decay of the mesons [3]. One of the observable related $b \to s$ transitions received many attentions is the branching ratio $B_{s\gamma}$ and the photon energy spectrum of the inclusive radiative decay $\bar{B} \to X_s\gamma$ (where B denotes B^0 or B^+) or equivalently $b \to s\gamma$ at quark level. The HFLAV group has obtained the world average result by combining the measurements from CLEO, BaBar and Belle [32], $B^{\text{exp}}_{s\gamma} = (3.49 \pm 0.19) \times 10^{-4}$ for a photon-energy cut-off $E_\gamma > 1.6$ GeV. This result is in good agreement with the newest updated SM prediction up to Next-to-Next-to-Leading Order (NNLO) $B^{\text{SM}}_{s\gamma} = (3.40 \pm 0.17) \times 10^{-4}$ [33], with the same E_γ energy cut-off. This leads to very strong constraints on the parameter space of New Physics (NP) model. Hence, we are going to consider the $b \to s\gamma$ decay in the 3-4-1-1 model.

2. The radiative decay

In the 3-4-1-1 model, the electroweak gauge group is extended to $SU(4)_L \otimes U(1)_X \otimes U(1)_N$. The electric charge Q and $B-L$ are defined as follows [20,21]

$$Q = T_3 + \beta T_8 + \gamma T_{15} + X, \qquad B-L = bT_8 + cT_{15} + N, \tag{1}$$

where the coefficients β, γ, b, c are determined by the charge parameters q, p, n, m as

$$\beta = -\frac{1}{\sqrt{3}}(2q+1), \qquad \gamma = \frac{1}{\sqrt{6}}(q-3p-1),$$
$$b = -\frac{2}{\sqrt{3}}(n+1), \qquad c = \frac{1}{\sqrt{6}}(n-3m-2). \tag{2}$$

The fermion and scalar contents in the 3-4-1-1 model are presented in Table 1 The vacuum expectation values (VEVs), $<\eta^0_1>= \frac{u}{\sqrt{2}}, <\rho^0_2>= \frac{v}{\sqrt{2}}, <\chi^0_3>= \frac{w}{\sqrt{2}}, <\Xi^0_4>= \frac{V}{\sqrt{2}}, <\phi>= \frac{\Lambda}{\sqrt{2}}$, break electroweak group into the $U(1)_{em} \otimes P$ with $P = P_n \otimes P_m$. The partial parities P_n, P_m can have values of 1 or $P^{\pm}_n = (-1)^{\pm(3n+1)}$, $P_m = (-1)^{\pm(3m+1)}$. Each $P_{n,m}$ corresponds to the Z_2 discrete symmetry, and thus $P = Z_2 \otimes Z_2$ is called doublet matter parity and classifies the particles into the normal particles, $P = (1,1)$ and the wrong particles, $P = (+,-),(-,+),(-,-)$. Two-component

Table 1. Particle content in the 3-4-1-1 model, where $a = 1,2,3$ and $\alpha = 1,2$.

Name	3-4-1-1 representation	Components	# flavors
ψ_{aL}	$\left(\mathbf{1},\mathbf{4},\frac{p+q-1}{4},\frac{m+n-2}{4}\right)$	$(\nu\ e\ E\ F)^T_{aL}$	3
ν_{aR}	$(\mathbf{1},\mathbf{1},0,-1)$		3
e_{aR}	$(\mathbf{1},\mathbf{1},-1,-1)$		3
$Q_{\alpha L}$	$\left(\mathbf{3},\mathbf{4}^*,-\frac{p+q+1/3}{4},-\frac{m+n+2/3}{4}\right)$	$(d\ -u\ J\ K)^T_{\alpha L}$	2
Q_{3L}	$\left(\mathbf{3},\mathbf{4},\frac{p+q+5/3}{4},\frac{m+n+10/3}{4}\right)$	$(u\ d\ J\ K)^T_{3L}$	2
u_{aR}	$\left(\mathbf{3},\mathbf{1},\frac{2}{3},\frac{1}{3}\right)$		3
d_{aR}	$\left(\mathbf{3},\mathbf{1},-\frac{1}{3},\frac{1}{3}\right)$		3
$J_{\alpha R}$	$(\mathbf{3},\mathbf{1},-q-1/3,-n-2/3)$		2
J_{3R}	$(\mathbf{3},\mathbf{1},q+2/3,n+4/3)$		1
$K_{\alpha R}$	$(\mathbf{3},\mathbf{1},-p-1/3,-m-2/3)$		2
K_{3R}	$(\mathbf{3},\mathbf{1},p+2/3,m+4/3)$		1
E_{aR}	$(\mathbf{1},\mathbf{1},q,n)$		3
F_{aR}	$(\mathbf{1},\mathbf{1},p,m)$		3
η	$\left(\mathbf{1},\mathbf{4},\frac{p+q-1}{4},\frac{m+n+2}{4}\right)$	$\left(\eta_1^0\ \eta_2^-\ \eta_3^q\ \eta_4^p\right)^T$	1
χ	$\left(\mathbf{1},\mathbf{4},\frac{p-3q-1}{4},\frac{m-3n-2}{4}\right)$	$\left(\chi_1^{-q}\ \chi_2^{-q-1}\ \chi_3^0\ \chi_4^{p-q}\right)^T$	1
ρ	$\left(\mathbf{1},\mathbf{4},\frac{q+p+3}{4},\frac{m+n+2}{4}\right)$	$\left(\rho_1^+\ \rho_2^0\ \rho_3^{q+1}\ \rho_4^{p+1}\right)^T$	1
Ξ	$\left(\mathbf{1},\mathbf{4},\frac{q-3p-1}{4},\frac{n-3m-2}{4}\right)$	$\left(\Xi_1^{-p}\ \Xi_2^{-p-1}\ \Xi_3^{q-p}\ \Xi_4^0\right)^T$	1
ϕ	$(\mathbf{1},\mathbf{1},0,2)$		1

DM scenarios can be obtained from candidates which are colorless and have electric neutrality for P_n and P_m odd fields. The interaction terms and the mass spectrum of particles are considered in [21]. Here, we list the interactions which give contributions to the $b \to s\gamma$ decay process.

- The singly charged Higgs, $\mathscr{H}_1^\pm$, couples to the SM quarks and creates the scalar flavor-changing charged currents. In the physical basis, we obtain the following Lagrangian

$$\mathscr{L}^{\mathscr{H}_1^\pm}_{\text{Yukawa}} = \frac{g}{\sqrt{2}m_W}\left\{\bar{d}'_L \mathscr{X} \mathscr{M}_u u'_R + \bar{d}'_R \mathscr{M}_d \mathscr{Y} u'_L\right\}\mathscr{H}_1^- + H.c., \tag{3}$$

where $\mathscr{Y} = t_{\alpha_2} V^\dagger_{\text{CKM}} - \frac{2}{s_{2\alpha_2}}\mathscr{T}$ and $\mathscr{X} = \frac{1}{t_{\alpha_2}} V^\dagger_{\text{CKM}} - \frac{2}{s_{2\alpha_2}}\mathscr{T}$. The $\mathscr{T}$ is defined as $\mathscr{T}_{ij} = (V^\dagger_{d_L})_{i3}(V_{u_L})_{3j}$, $s_{2\alpha_2} = \sin 2\alpha_2, t_{2\alpha_2} = \tan 2\alpha_2 = \frac{v}{u}$.

- Other charged Higgs, $\mathscr{H}_{2,3}^{\pm q,p}$, $\mathscr{H}_{4,5}^{\pm(q+1),(p+1)}$, interact to both SM quarks and exotic quark as follows:

$$\mathscr{L}_{\text{Yukawa}}^{\mathscr{H}_{2,3},\mathscr{H}_{4,5}} = -\frac{g}{\sqrt{2}m_W c_{\alpha_2}}\left\{\bar{J}'_{\alpha L}(V_L^d)_{\alpha a}\mathscr{M}_d d'_{aR}\mathscr{H}_2^{-q} + \bar{K}'_{\alpha L}(V_L^d)_{\alpha a}\mathscr{M}_d d'_{aR}\mathscr{H}_3^{-p}\right\}$$
$$+\frac{g}{\sqrt{2}m_W s_{\alpha_2}}\left\{\bar{J}'_{3L}(V_L^d)_{3a}\mathscr{M}_d d'_{aR}\mathscr{H}_4^{q+1} + \bar{K}'_{3L}(V_L^d)_{3a}\mathscr{M}_d d'_{aR}\mathscr{H}_5^{p+1}\right\} + H.c. \quad (4)$$

- The charged currents associated $W_{13}^{\pm q}, W_{14}^{\pm p}, W_{23}^{\pm(q+1)}$ and $W_{24}^{\pm(p+1)}$ are expressed by

$$\mathscr{L}_{W_{13,14},W_{23,24}}^{\text{quark}} = \frac{g}{\sqrt{2}}(\bar{d}'_{iL}(V_{d_L})^*_{i\alpha}\gamma^\mu J'_{\alpha L}W_{13\mu}^q + \bar{d}'_{iL}(V_{d_L})^*_{i\alpha}\gamma^\mu K'_{\alpha L}W_{14\mu}^p$$
$$-\bar{J}'_{3L}\gamma^\mu(V_{d_L})_{3i}d'_{iL}W_{23\mu}^{q+1} - \bar{K}'_{3L}\gamma^\mu(V_{d_L})_{3i}d'_{iL}W_{24\mu}^{p+1}) + H.c. \quad (5)$$

- The remaining contributions to the studying decay come from the FCNCs coupled by both new neutral gauge boson $Z_{2,3}$ and new scalars $H_1, \mathscr{A}$. These interactions have been extensively studied in [31] and shown that FCNCs induced by $Z_{2,3}$ are more dominant, in comparison with FCNCs induced by $H_1, \mathscr{A}$. Therefore, we only consider FCNC sources induced by Z_2 and Z_3. Their relevant Lagrangian is

$$\mathscr{L}_{Z_{2,3}}^{\text{FCNC}} = (V_{qL}^*)_{3i}(V_{qL})_{3j}(g_2 Z_{2\mu} + g_3 Z_{3\mu})\bar{q}'_{iL}\gamma^\mu q'_{jL}, \quad i \neq j, \quad (6)$$

where

$$g_2 = \frac{g}{\sqrt{6}}\left(\frac{\sqrt{2}}{\sqrt{1-\beta^2 t_W^2}}c_\phi - \frac{1+\gamma(\sqrt{2}\beta+\gamma)t_X^2}{\sqrt{1+\gamma^2 t_X^2}}\right),\ g_3 = g_2(c_\phi \to s_\phi, s_\phi \to -c_\phi), \quad (7)$$

with ϕ is the mixing angle between Z_2 and Z_3 and determined by

$$t_{2\phi} = \frac{4\sqrt{2}w^2[1-\gamma(2\sqrt{2}\beta-\gamma)t_X^2]\sqrt{1+(\beta^2+\gamma^2)t_X^2}}{w^2[7-\gamma^2(2\sqrt{2}\beta-\gamma)^2 t_X^4 + (8\beta^2+4\sqrt{2}\beta\gamma+6\gamma^2)t_X^2] - 9V^2(1+\gamma^2 t_X^2)^2}. \quad (8)$$

We would like to emphasize that details of the physical states of charged Higgs $\mathscr{H}_1^{\pm}$, $\mathscr{H}_2^{\pm q}$, $\mathscr{H}_3^{\pm p}$, $\mathscr{H}_4^{\pm(q+1)}$, $\mathscr{H}_5^{\pm(p+1)}$, as well as new non-hermitian physical gauge bosons $W_{13}^{\pm q}$, $W_{14}^{\pm p}, W_{23}^{\pm(q+1)}$, $W_{24}^{\pm(p+1)}$, and new neutral gauge bosons, $Z_{2,3}$, can be found in [21]. In the fermion sector, the matrices can be diagonalized by both the matrices as

$$V_{u_L}^\dagger m^u V_{u_R} = \mathscr{M}_u = \text{Diag}(m_{u_1}, m_{u_2}, m_{u_3}), \quad V_{d_L}^\dagger m^d V_{d_R} = \mathscr{M}_d = \text{Diag}(m_{d_1}, m_{d_2}, m_{d_3}), \quad (9)$$

and the relations between mass eigenstates and flavor states are given by

$$u'_{L,R} = (u'_{1L,R}, u'_{2L,R}, u'_{3L,R})^T = V_{u_{L,R}}^\dagger (u_{1L,R}, u_{2L,R}, u_{3L,R})^T,$$
$$d'_{L,R} = (d'_{1L,R}, d'_{2L,R}, d'_{3L,R})^T = V_{d_{L,R}}^\dagger (d_{1L,R}, d_{2L,R}, d_{3L,R})^T. \quad (10)$$

The CKM matrix is defined as $V_{\text{CKM}} = V_{u_L}^\dagger V_{d_L}$. The exotic quarks have heavy masses at TeV scale. They do not mix with SM quarks and are physical fields themselves.

The effective Hamiltonian for the decay $b \to s\gamma$ is expressed by

$$\mathscr{H}_{\text{eff}}^{b\to s\gamma} = -\frac{4G_F}{\sqrt{2}}V_{tb}V_{ts}^*[C_7(\mu_b)\mathscr{O}_7 + C_8(\mu_b)\mathscr{O}_8 + C'_7(\mu_b)\mathscr{O}'_7 + C'_8(\mu_b)\mathscr{O}'_8], \quad (11)$$

with $\mu_b = \mathcal{O}(m_b)$ is the energy scale of the decay $b \to s\gamma$. The electromagnetic and chromomagnetic dipole operators $\mathcal{O}_7, \mathcal{O}_8$ are defined as

$$\mathcal{O}_7 = \frac{e}{(4\pi)^2} m_b(\bar{s}_\alpha \sigma_{\mu\nu} P_R b_\alpha) F^{\mu\nu}, \quad \mathcal{O}_8 = \frac{g_s}{(4\pi)^2} m_b(\bar{s}_\alpha \sigma_{\mu\nu} T^a_{\alpha\beta} P_R b_\beta) G^{a\mu\nu}, \tag{12}$$

and the primed operators $\mathcal{O}'_{7,8}$ are obtained by replacing $P_L \leftrightarrow P_R$. The primed Wilson coefficients (WCs) $C'_{7,8}$ are suppressed by the ratio m_s/m_b, we ignore them from our calculation. The charged scalar currents given in Eq. (4) only contribute to the $C'_{7,8}$, and are ignored for the $b \to s\gamma$ decay. The WCs $C_{7,8}(\mu_b)$ split as the sum of the SM and NP contributions

$$C_{7,8}(\mu_b) = C^{\rm SM}_{7,8}(\mu_b) + C^{\rm NP}_{7,8}(\mu_b), \tag{13}$$

with $C^{\rm SM}_{7,8}$ are the SM WCs which are first given by [34], at the scale $\mu \sim m_W$

$$C_7^{\rm SM(0)}(m_W) = \frac{m_t^2}{m_W^2} f_\gamma\left(\frac{m_t^2}{m_W^2}\right), \quad C_8^{\rm SM(0)}(m_W) = \frac{m_t^2}{m_W^2} f_g\left(\frac{m_t^2}{m_W^2}\right), \tag{14}$$

where the index 0 indicates that the WCss are calculated without QCD correction. The NP contributions to the WCs , $C^{\rm NP}_{7,8}$, come from charged scalar (vector) currents given in Eqs. (3) (5), and the FCNCs given in Eq. (6). We draw the Feymann diagrams in Fig. 1 from these interactions, which contribute to the $b \to s\gamma$ at the one loop level, and divide the contributions as follows:

$$C^{\rm NP(0)}_{7,8} = C^{\mathcal{H}_1(0)}_{7,8}(m_{\mathcal{H}_1}) + C^{W_{13,14,23,24}}_{7,8}(m_{W_{13,14,23,24}}) + C^{Z_{2,3}(0)}_{7,8}(m_{Z_{2,3}}), \tag{15}$$

where

$$\begin{aligned}
C_7^{\mathcal{H}_1(0)}(m_{\mathcal{H}_1}) &= \frac{m_t^2}{m_{\mathcal{H}_1}^2}\left[\frac{1}{3}t_{\alpha_2}^2 f_\gamma\left(\frac{m_t^2}{m_{\mathcal{H}_1}^2}\right) + f'_\gamma\left(\frac{m_t^2}{m_{\mathcal{H}_1}^2}\right)\right],\\
C_8^{\mathcal{H}_1(0)}(m_{\mathcal{H}_1}) &= \frac{m_t^2}{m_{\mathcal{H}_1}^2}\left[\frac{1}{3}t_{\alpha_2}^2 f_g\left(\frac{m_t^2}{m_{\mathcal{H}_1}^2}\right) + f'_g\left(\frac{m_t^2}{m_{\mathcal{H}_1}^2}\right)\right],\\
C_7^{V(0)}(m_V) &= \frac{V^*_{\alpha s}V_{\alpha b}}{V^*_{ts}V_{tb}}\frac{m_W^2}{m_V^2}\frac{m_{F_\alpha}^2}{m_V^2}\left[Q_{F_\alpha} h_\gamma\left(\frac{m_{F_\alpha}^2}{m_V^2}\right) + Q_V j_\gamma\left(\frac{m_{F_\alpha}^2}{m_V^2}\right)\right],\\
C_8^{V(0)}(m_V) &= \frac{V^*_{\alpha s}V_{\alpha b}}{V^*_{ts}V_{tb}}\frac{m_W^2}{m_V^2}\frac{m_{F_\alpha}^2}{m_V^2} f_g\left(\frac{m_{F_\alpha}^2}{m_V^2}\right),\\
C_7^{V'(0)}(m_{V'}) &= \frac{m_W^2}{m_{V'}^2}\frac{m_{F_3}^2}{m_{V'}^2}\left[Q_{F_3} h_\gamma\left(\frac{m_{F_3}^2}{m_{V'}^2}\right) + Q_{V'} j_\gamma\left(\frac{m_{F_3}^2}{m_{V'}^2}\right)\right],\\
C_8^{V'(0)}(m_{V'}) &= \frac{m_W^2}{m_{V'}^2}\frac{m_{F_3}^2}{m_{V'}^2} f_g\left(\frac{m_{F_3}^2}{m_{V'}^2}\right),
\end{aligned} \tag{16}$$

where we denote

$$\begin{aligned}
V &= W_{13}, W_{14}, \quad F_\alpha = J_\alpha, K_\alpha, \quad Q_{F_\alpha} = q - \frac{1}{3}, p - \frac{1}{3}, \quad Q_V = q, p,\\
V' &= W_{23}, W_{24}, \quad F_3 = J_3, K_3, \quad Q_{F_3} = q + \frac{2}{3}, p + \frac{2}{3}, \quad Q_{V'} = q+1, p+1.
\end{aligned} \tag{17}$$

The functions $f_{\gamma,g}$ and $f'_{\gamma,g}$ are defined by

$$f_\gamma(x) = \frac{(7-5x-8x^2)}{24(x-1)^3} + \frac{x(3x-2)}{4(x-1)^4}\ln x, \quad f'_\gamma(x) = \frac{(3-5x)}{12(x-1)^2} + \frac{(3x-2)}{6(x-1)^3}\ln x,$$
$$f_g(x) = \frac{2+5x-x^2}{8(x-1)^3} - \frac{3x}{4(x-1)^4}\ln x, \quad f'_g(x) = \frac{3-x}{4(x-1)^2} - \frac{1}{2(x-1)^3}\ln x,$$
$$h_\gamma = \frac{-2-5x+x^2}{8(x-1)^3} + \frac{3x^2}{4(x-1)^4}\ln x, \quad j_\gamma = \frac{-1+5x+2x^2}{8(x-1)^3} - \frac{3x^3}{4(x-1)^4}\ln x. \tag{18}$$

The $C_7^{Z_{2,3}(0)}(m_{Z_{2,3}})$ are obtained by the FCNCs coupled to the $Z_{2,3}$ and have a form as given in [35]

$$C_7^{Z_{2,3}(0)}(m_{Z_{2,3}}) = -\frac{2}{9g^2}\frac{m_W^2}{m_{Z_{2,3}}^2}\sum_{f=d,s,b}\frac{g_L^{fs*}g_L^{fb}}{V_{ts}^*V_{tb}} + \frac{2}{3g^2}\frac{m_W^2}{m_{Z_{2,3}}^2}\sum_{f=d,s,b}\frac{m_f}{m_b}\frac{g_L^{fs*}g_R^{fb}}{V_{ts}^*V_{tb}},$$
$$C_8^{Z_{2,3}(0)}(m_{Z_{2,3}}) = -3C_7^{Z_{2,3}}(m_{Z_{2,3}}). \tag{19}$$

The flavor couplings, $g_{L,R}^{ff} = [g_V^{Z_{2,3}}(f) \pm g_A^{Z_{2,3}}(f)]/2$, can be found in [21], and the flavor-violating couplings, $g^{fs,fb}$, are defined in Eq. (6).

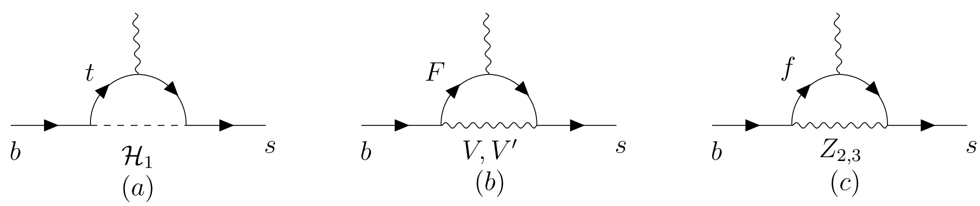

Fig. 1. The one-loop diagrams induced by new particles of the 3-4-1-1 model contributing to $b \to s\gamma$ decay. Diagrams (a), (b) and (c) are for Wilson coefficients $C_7^{\mathcal{H}_1}$, $C_7^{V,V'}$ and $C_7^{Z_{2,3}}$, respectively. Here we use notations in Eq. (17) for F and V, V', where f stands for down-type quarks d, s, b.

In fact, the QCD corrections to $b \to s\gamma$ is necessary for the analysis. In SM, $C_{7,8}^{\text{SM}}$ were calculated up to Next-to-Next-Leading Order (NNLO), specifically, $C_7^{\text{SM}}(\mu_b) = -0.3636$ for $\mu_b = 2.0$ GeV [33, 36, 37]. However, the NP contributions to the $C_{7,8}^{\text{NP}}$ have been considered at the Leading Order (LO) [35, 38]. In this work, we study the effect of QCD corrections on the $C_{7,8}^{\text{NP}}$ at the LO. There are several heavy scales: $m_{Z_{2,3}}$, $m_{\mathcal{H}_1}$ and $m_{W_{13,14,23,24}}$ in the 3-4-1-1 model. At high energies, the QCD running affects insignificantly and the difference among these large scales can be ignored. Hence, we propose all calculations are at the same scale and we choose $\mu \sim m_{\mathcal{H}_1}$. The QCD corrections for $C_7^{Z_{2,3}}$ are given by

$$C_7^{Z_{2,3}}(\mu_b) = \kappa_7 C_7^{Z_{2,3}}(m_{\mathcal{H}_1}) + \kappa_8 C_8^{Z_{2,3}}(m_{\mathcal{H}_1}) + \Delta_{Z_{Z_{2,3}}}(\mu_b), \tag{20}$$

where $\kappa_{7,8}$ are NP magic numbers $\kappa_7 = 0.39, \kappa_8 = 0.130$ at $\mu \sim 10$ TeV [38]. $\Delta_{Z_{Z_{2,3}}}(\mu_b)$ are the contributions coming from the mixing of new neutral current-current operators, generated by the exchange of $Z_{2,3}$ with the dipole operators $\mathscr{O}_{7,8}$

$$\Delta_{Z_{Z_{2,3}}}(\mu_b) = \sum_{\substack{A=L,R,\\ f=u,c,t,d,s,b}} \kappa^f_{LA}\Delta_{LA}C^f_2(w) + \sum_{A=L,R} \hat{\kappa}^d_{LA}\Delta_{LA}\hat{C}^d_2(w),$$

$$\Delta_{LA}C^f_2(m_{\mathscr{H}_1}) = -\frac{2}{g^2}\frac{g^{sb*}_L g^{ff}_A}{V^*_{ts}V_{tb}}, \quad \Delta_{LA}\hat{C}^d_2(m_{\mathscr{H}_1}) = -\frac{2}{g^2}\frac{g^{sd*}_L g^{bd}_A}{V^*_{ts}V_{tb}}. \tag{21}$$

If including the LO of QCD corrections, $C_7^{\mathscr{H}_1}$ and $C_7^{V,V'}(\mu_b)$ have the forms as [35], [38]

$$\begin{aligned}
C_7^{\mathscr{H}_1}(\mu_b) &= \kappa_7 C_7^{\mathscr{H}_1}(m_{\mathscr{H}_1}) + \kappa_8 C_8^{\mathscr{H}_1}(m_{\mathscr{H}_1}),\\
C_7^{V}(\mu_b) &= \kappa_7 C_7^{V}(m_{\mathscr{H}_1}) + \kappa_8 C_8^{V}(m_{\mathscr{H}_1}),\\
C_7^{V'}(\mu_b) &= \kappa_7 C_7^{V'}(m_{\mathscr{H}_1}) + \kappa_8 C_8^{V'}(m_{\mathscr{H}_1}).
\end{aligned} \tag{22}$$

The branching ratio for the considering decay is given as [38]

$$B_{s\gamma} = \frac{6\alpha_{\text{em}}}{\pi C}\frac{|V^*_{ts}V_{tb}|^2}{|V_{cb}|^2}(|C_7(\mu_b)|^2 + N(E_\gamma))\text{Br}(\bar{B}\to X_c l\bar{\nu}), \tag{23}$$

where $N(E_\gamma)$ is a non-perturbative contribution which amounts around 4% of the branching ratio, $N(E_\gamma) \simeq 3.3\times 10^{-3}$ [33], C is the semileptonic phase-space factor $C = |V_{ub}/V_{cb}|^2\Gamma(\bar{B}\to X_c e\bar{\nu}_e)/\Gamma(\bar{B}\to X_u e\bar{\nu}_e) = 0.567(7)(10)$, see in [39]. The branching ratio for semi-leptonic decay $\text{Br}(\bar{B}\to X_c l\bar{\nu}) = 0.1067(16)$ [40].

The $B_{s\gamma}$ is predicted as a function of the masses of new particles, namely, $m_{\mathscr{H}_1}$, $m_{W_{13,14,23,24}}$ and $m_{J_\alpha,K_\alpha,J_3,K_3}$, in the 3-4-1-1 model. The masses of new particles can be evaluated in the limit $w = V \gg u, v$, as follows

$$\begin{aligned}
m_{W_{13,14,23,24}} &\equiv m_V \simeq gw/2 \simeq 0.32w, \quad g = \frac{\sqrt{4\pi\alpha}}{s_W} \simeq 0.64\\
m^2_{\mathscr{H}_1} &\simeq -\lambda_{17}\frac{u^2+v^2}{2uv}wV \equiv -\frac{\lambda_{17}w^2}{2}\left(t_{\alpha_2} + \frac{1}{t_{\alpha_2}}\right).
\end{aligned} \tag{24}$$

The masses of new quarks $F \equiv J_\alpha, K_\alpha, J_3, K_3$ are large and depend on completely unknown Yukawa couplings $h^{J,K}_{\alpha,3}$. These masses only have effect on $C^{V,V'}_{7,8}$ via the mass hierarchy ratios $\frac{m^2_F}{m^2_V}$.

We first estimate the effect of each kind of diagrams given in Fig.(1) on the $B_{s\gamma}$.

- The contributions from diagrams (a) of Fig. (1) are expected to be strongly dependent on $t_{2\alpha}$ and the mass of the singly charged Higgs. This contribution is significant in the limit of larger value of $t_{2\alpha}$, and even can be equivalent to that of the SM if $m^2_{\mathscr{H}_1} \simeq t^2_{2\alpha}m^2_W$.
- If the following condition is met, $\frac{m^2_F}{m^2_V} \simeq \frac{m^2_t}{m^2_W}$, the contributions obtained from the diagram (b) of the Fig.(1) are suppressed by a factor $\frac{m^2_W}{m^2_V}$ when compared to the SM. Otherwise, if $\frac{m^2_F}{m^4_V} \simeq \epsilon\frac{m^2_t}{m^4_W}$, we expect the contribution of this type of diagram to be similar to that of the SM.

- If NP scale is a few TeV, we estimate $C_7^{Z_{2,3}}(\mu_b) \simeq \mathcal{O}(10^{-5})$, which is strongly suppressed by the SM prediction, $C_7^{\rm SM}(\mu_b = 2\ \text{GeV}) = -0.3636$. Therefore, we can safely eliminate $C_7^{Z_{2,3}}$.

The input parameters are listed in the Table (2).

Table 2. The numerical values of input parameters.

Input parameters	Values	Input parameters	Values
$N(E_\gamma)$	3.3×10^{-3} [33]	$\lvert V_{ts}^* V_{tb}/V_{cb}\rvert^2$	$0.9626(12)$ [40]
$\text{Br}(\bar{B} \to X_c l \bar{\nu})$	$0.1067(16)$ [40]	V_{us}	$0.22514(55)$ [41]
$m_{t,\text{pole}}$	$173.21(51)(71)$ GeV [40]	V_{ub}	$0.00365(10)e^{-i(66.8(2))^\circ}$ [41]
$\alpha_{\text{em}}(0)$	$1/137.036(21)$ [40]	V_{cs}	$0.97344(12)e^{-i(001880(52))^\circ}$ [41]
C	$0.57(7)(10)$ [39]	V_{cb}	$0.04241(65)$ [41]
$C_7^{\rm SM}(\mu_b = 2.0\ \text{GeV})$	-0.3636 [33, 36, 37]	V_{ts}	$-0.04124(56)e^{i(1.056(32))^\circ}$ [41]
m_W	80.3875 GeV [40]	V_{tb}	$0.999112(24)$ [41]

It is important to mention that the strongest bound of the new physics scales can be obtained from the $B_s^0 - \bar{B}_s^0$ mixing, $w = V > 25$ TeV, given by [31]. Next, we perform a numerical study to evaluate the contribution of NP in the $Br_{s\gamma}$ in detail, thus we can constrain free parameters related to this observable, namely the Higgs coupling λ_{17}, the mixing angle t_{α_2} and the dimensionless ratio $\epsilon = \frac{m_F^2/m_V^4}{m_t^2/m_W^4}$.

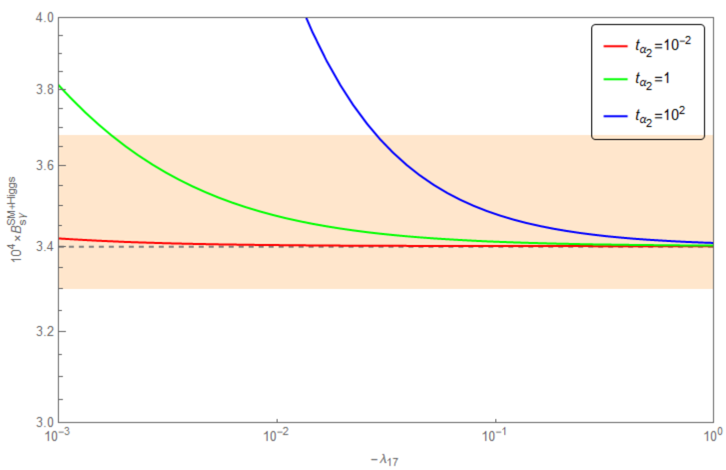

Fig. 2. The dependence of $B_{s\gamma}$ on λ_{17} with fixing $w = V = 26$ TeV and when only $C_7^{\mathscr{H}_1}$ accounting. The orange band highlights the experimental world average $B_{s\gamma}^{\rm exp} = (3.49 \pm 0.19) \times 10^{-4}$ [32], whereas the dashed gray line indicates the central value of the SM prediction $B_{s\gamma}^{\text{SM-central}} = 3.4 \times 10^{-4}$.

In Fig. 2, we study the dependence of $B_{s\gamma}$ on the Higgs coupling λ_{17} in the case where only $C_7^{\mathscr{H}_1}$ contributes and t_{α_2} is fixed at $10^{-2}, 1$ and 10^2. As shown in this figure, $B_{s\gamma}$ is strongly affected by t_{α_2}. We see that when $t_{\alpha_2} = 10^{-2}$ (red line), $B_{s\gamma}$ almost consistent with the central value of the SM prediction $B_{s\gamma}^{\text{SM-central}} = 3.4 \times 10^{-4}$ [33], whereas the predicted branching ratio is larger for high values of $t_{\alpha_2} = 1$ or $t_{\alpha_2} = 10^2$. This occurs because in the low t_{α_2}, we have $m^2_{\mathscr{H}_1} \simeq \frac{w^2}{2t_{\alpha_2}}$, resulting in a very small Wilson coefficient $C_7^{\mathscr{H}_1} \simeq \frac{t^2_{\alpha_2}}{m^2_{\mathscr{H}_1}} = \frac{t^3_{\alpha_2}}{w^2} \ll C_7^{\text{SM}}$. In contrast, $m^2_{\mathscr{H}_1} \simeq w^2 t_{\alpha_2}$ for high t_{α_2}, the Wilson coefficient becomes $C_7^{\mathscr{H}_1} \simeq \frac{t_{\alpha_2}}{w^2}$, significantly increasing to $B_{s\gamma}$. The figure also suggests that as the value of t_{α_2} increases, the appropriate value of λ_{17} decreases. For example, we obtain the limits of λ_{17} as $-\lambda_{17} \geq 2.8 \times 10^{-2}$ for $t_{\alpha_2} = 10^2$ and $-\lambda_{17} \geq 1.7 \times 10^{-3}$ for $t_{\alpha_2} = 1$, respectively. In order to see the interdependence between t_{α_2} and λ_{17} in general, we draw the contour in Fig. 3.

Next, we study the scenario when only the new gauge bosons V, V' contribute $B_{s\gamma}$. We plot the branching ratio as a function of the dimensionless ratio $\epsilon = \frac{m_F^2/m_V^4}{m_t^2/m_W^4} = \frac{8h_F^2/(g^4w^2)}{m_t^2/m_W^4}$. It is worth noting that the Yukawa coupling h_F should be constrained by the perturbative condition $h_F^2/(4\pi) \leq 1$. For $m_t = 173$ GeV, $m_W = 0.4$ GeV [3], $g \simeq 0.64$ and $w = 26$ TeV, we obtain the upper limit of $\epsilon \leq 1.2 \times 10^{-3}$. For instance, we can choose the range $\epsilon \in [10^{-6}, 10^{-3}]$.

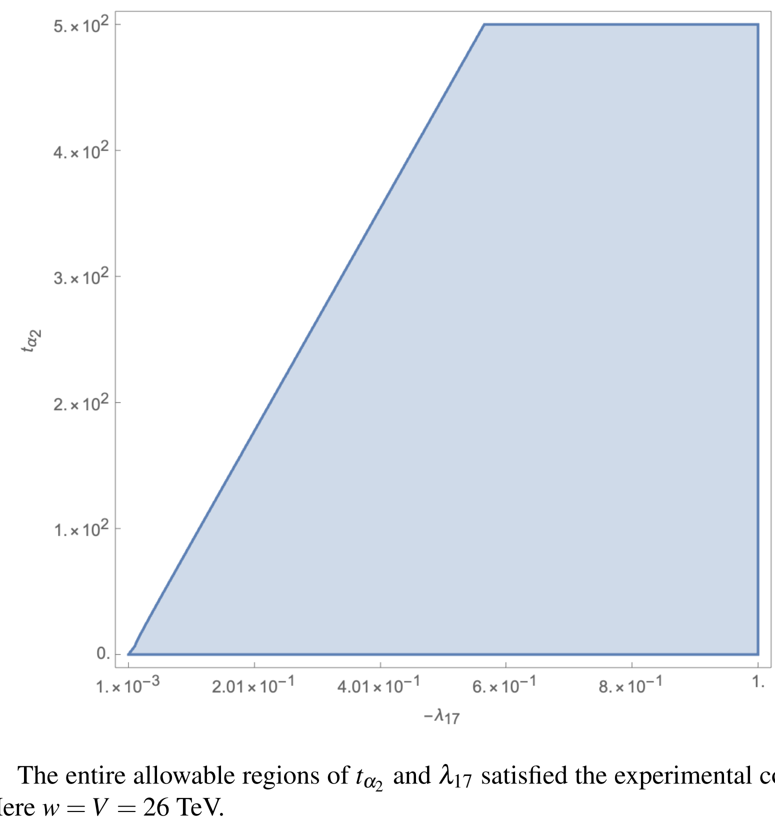

Fig. 3. The entire allowable regions of t_{α_2} and λ_{17} satisfied the experimental constrains [32]. Here $w = V = 26$ TeV.

Figure 4 plots $B_{s\gamma}$ as a function of ϵ when only considering Wilson coefficients $C_7^{V,V'}$ contributions and choosing different values of two charge parameters p,q. We see that the branching ratio in this scenario does not depend on ϵ and values of p,q. With the condition $w = V > 25$ TeV [31], the branching ratio is consistent with the central value of SM prediction, implying that the contribution of new gauge bosons V,V' in diagram (b) of Fig. (1) are very tiny. To conclude, we draw Fig. 5 to illustrate the magnitude of each NP's contribution to the branching ratio. Here we set NP's contributions depending on coupling λ_{17}, and we fix $t_{\alpha_2} = 1, p = q = 0$ and $\epsilon = 5 \times 10^{-4}$. The charged Higgs boson $\mathscr{H}_1^{\pm}$ makes the most significant contribution, whereas new gauge bosons V,V' are insignificant.

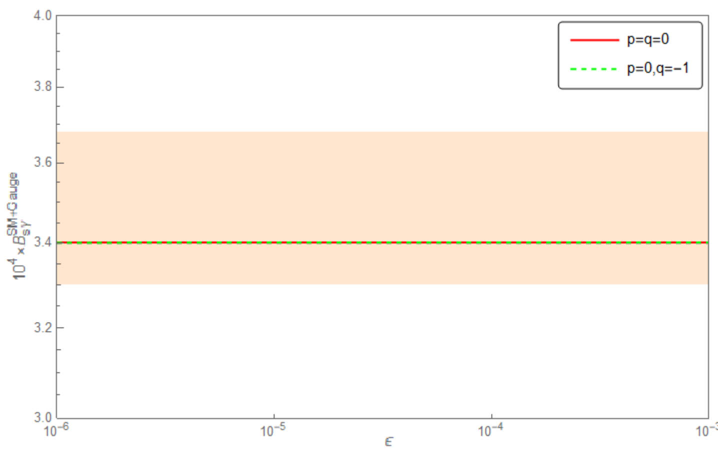

Fig. 4. The dependence of $B_{s\gamma}$ on ϵ with fixing $w = V = 26$ TeV and when only $C_7^{V,V'}$ accounting. The orange band highlights the experimental world average $B_{s\gamma}^{\text{exp}} = (3.49 \pm 0.19) \times 10^{-4}$ [32], whereas the dashed gray line indicates the central value of the SM prediction $B_{s\gamma}^{\text{SM-central}} = 3.4 \times 10^{-4}$.

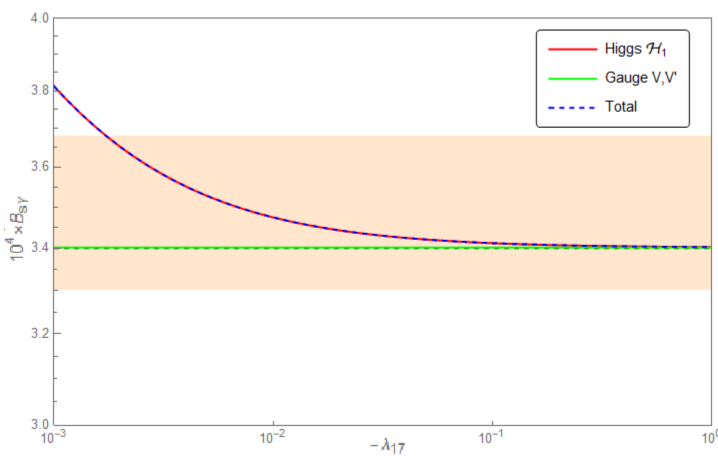

Fig. 5. The comparison between each NP contributions to $B_{s\gamma}$. The orange band highlights the experimental world average $B_{s\gamma}^{\text{exp}} = (3.49 \pm 0.19) \times 10^{-4}$ [32], whereas the dashed gray line indicates the central value of the SM prediction $B_{s\gamma}^{\text{SM-central}} = 3.4 \times 10^{-4}$. Here $t_{\alpha_2} = 1, p = q = 0$ and $\epsilon = 5 \times 10^{-4}$.

3. Conclusions

In short, the branching ratio of weak inclusive decay $b \to s\gamma$ has been investigated in the 3-4-1-1 model with arbitrary charge parameters p, q. We show that among the NP contributions, the new singly charged Higgs boson $\mathscr{H}_1^{\pm}$ gives mostly to the $B_{s\gamma}$, while other new boson, namely $\mathscr{H}_2^{\pm q}, \mathscr{H}_3^{\pm p}, \mathscr{H}_4^{\pm(q+1)}, \mathscr{H}_5^{\pm(p+1)}$ and new gauge $W_{13}^{\pm q}$, $W_{14}^{\pm p}, W_{23}^{\pm(q+1)}, W_{24}^{\pm(p+1)}$ contribute the least. Furthermore, the contributions by FCNCs associated with new neutral gauge bosons $Z_{2,3}$ to Wilson coefficients $C_7^{Z_{2,3}}(\mu_b)$ are much smaller than the SM contribution $C_7^{\mathrm{SM}}(\mu_b)$ and therefore will be ignored. Consequently, the $B_{s\gamma}$ is unaffected by the charge parameters p, q. The predicted branching ratio is influenced by the mixing angle t_{α_2} and the Higgs coupling λ_{17}, but will satisfy the world average experimental result [32] if the lower bounds of new physics scales $w = V > 25$ TeV are imposed from the $B - \bar{B}_s^0$ oscillation [31].

Acknowledgment

This work is supported by the International Physics Center, Institute of Physics with grant number ICP.2022.16.

Conflict of interest

The authors have no conflict of interest to declare.

References

[1] T. Kajita, *Nobel Lecture: Discovery of atmospheric neutrino oscillations*, Rev. Mod. Phys. **88** (2016) 030501.

[2] A. B. McDonald, *Nobel Lecture: The Sudbury Neutrino Observatory: Observation of flavor change for solar neutrinos*, Rev. Mod. Phys. **88** (2016) 030502.

[3] Particle Data Group Collaboration, *Review of Particle Physics*, PTEP **2022** (2022) 083C01.

[4] G. Jungman, M. Kamionkowski and K. Griest, *Supersymmetric dark matter*, Phys. Rept. **267** (1996) 195.

[5] G. Bertone, D. Hooper and J. Silk, *Particle dark matter: Evidence, candidates and constraints*, Phys. Rept. **405** (2005) 279.

[6] J. R. Ellis, J. S. Hagelin, D. V. Nanopoulos, K. A. Olive and M. Srednicki, *Supersymmetric Relics from the Big Bang*, Nucl. Phys. B **238** (1984) 453.

[7] E. W. Kolb and R. Slansky, *Dimensional Reduction in the Early Universe: Where Have the Massive Particles Gone?*, Phys. Lett. B **135** (1984) 378.

[8] T. Appelquist, H.-C. Cheng and B. A. Dobrescu, *Bounds on universal extra dimensions*, Phys. Rev. D **64** (2001) 035002.

[9] K. Agashe and G. Servant, *Warped unification, proton stability and dark matter*, Phys. Rev. Lett. **93** (2004) 231805.

[10] N. Arkani-Hamed, A. G. Cohen, E. Katz and A. E. Nelson, *The Littlest Higgs*, JHEP **07** (2002) 034.

[11] I. Low, *T parity and the littlest Higgs*, JHEP **10** (2004) 067.

[12] P. V. Dong, H. T. Hung and T. D. Tham, *3-3-1-1 model for dark matter*, Phys. Rev. D **87** (2013) 115003.

[13] D. T. Huong and P. V. Dong, *Neutrino masses and superheavy dark matter in the 3-3-1-1 model*, Eur. Phys. J. C **77** (2017) 204.

[14] D. Abercrombie *et al.*, *Dark Matter benchmark models for early LHC Run-2 Searches: Report of the ATLAS/CMS Dark Matter Forum*, Phys. Dark Univ. **27** (2020) 100371.

[15] C. Boehm, P. Fayet and J. Silk, *Light and heavy dark matter particles*, Phys. Rev. D **69** (2004) 101302.

[16] D. Chialva, P. S. B. Dev and A. Mazumdar, *Multiple dark matter scenarios from ubiquitous stringy throats*, Phys. Rev. D **87** (2013) 063522.

[17] M. Aoki, J. Kubo and H. Takano, *Two-loop radiative seesaw mechanism with multicomponent dark matter explaining the possible γ excess in the Higgs boson decay and at the Fermi LAT*, Phys. Rev. D **87** (2013) 116001.

[18] S. Bhattacharya, A. Drozd, B. Grzadkowski and J. Wudka, *Two-Component Dark Matter*, JHEP **10** (2013) 158.

[19] G. Arcadi, C. Gross, O. Lebedev, Y. Mambrini, S. Pokorski and T. Toma, *Multicomponent Dark Matter from Gauge Symmetry*, JHEP **12** (2016) 081.

[20] D. Van Loi, P. Van Dong and L. X. Thuy, *Kinetic mixing effect in noncommutative $B-L$ gauge theory*, JHEP **09** (2019) 054.

[21] C. H. Nam, D. Van Loi, L. X. Thuy and P. Van Dong, *Multicomponent dark matter in noncommutative $B-L$ gauge theory*, JHEP **12** (2020) 029.

[22] A. Ahmed, M. Duch, B. Grzadkowski and M. Iglicki, *Multi-Component Dark Matter: the vector and fermion case*, Eur. Phys. J. C **78** (2018) 905.

[23] S. Bhattacharya, P. Ghosh, A. K. Saha and A. Sil, *Two component dark matter with inert Higgs doublet: neutrino mass, high scale validity and collider searches*, JHEP **03** (2020) 090.

[24] J. Fan, A. Katz, L. Randall and M. Reece, *Double-Disk Dark Matter*, Phys. Dark Univ. **2** (2013) 139.

[25] J. Fan, A. Katz, L. Randall and M. Reece, *Dark-Disk Universe*, Phys. Rev. Lett. **110** (2013) 211302.

[26] K. Agashe, Y. Cui, L. Necib and J. Thaler, *(In)direct Detection of Boosted Dark Matter*, JCAP **10** (2014) 062.

[27] K. Kong, G. Mohlabeng and J.-C. Park, *Boosted dark matter signals uplifted with self-interaction*, Phys. Lett. B **743** (2015) 256.

[28] H. Alhazmi, K. Kong, G. Mohlabeng and J.-C. Park, *Boosted Dark Matter at the Deep Underground Neutrino Experiment*, JHEP **04** (2017) 158.

[29] O. D. Elbert, J. S. Bullock, S. Garrison-Kimmel, M. Rocha, J. Oñorbe and A. H. G. Peter, *Core formation in dwarf haloes with self-interacting dark matter: no fine-tuning necessary*, Mon. Not. Roy. Astron. Soc. **453** (2015) 29.

[30] S. Tulin and H.-B. Yu, *Dark Matter Self-interactions and Small Scale Structure*, Phys. Rept. **730** (2018) 1.

[31] D. T. Huong, L. X. Thuy, N. T. Nhuan and H. T. Phuong, *Investigation of the FCNC Processes in the 3-4-1-1 Model*, Comm. Phys. **31** (2021) 399.

[32] HFLAV Collaboration, *Averages of b-hadron, c-hadron, and τ-lepton properties as of 2021*, .

[33] M. Misiak, A. Rehman and M. Steinhauser, *Towards $\overline{B} \to X_s\gamma$ at the NNLO in QCD without interpolation in m_c*, JHEP **06** (2020) 175.

[34] T. Inami and C. S. Lim, *Effects of Superheavy Quarks and Leptons in Low-Energy Weak Processes $K_L \to \mu\bar{\mu}$, $K^+ \to \pi^+\nu\bar{\nu}$ and $K^0 \leftrightarrow \bar{K}^0$*, Prog. Theor. Phys. **65** (1981) 297.

[35] A. J. Buras, F. De Fazio, J. Girrbach and M. V. Carlucci, *The Anatomy of Quark Flavour Observables in 331 Models in the Flavour Precision Era*, JHEP **02** (2013) 023.

[36] M. Misiak and M. Steinhauser, *NNLO QCD corrections to the $\bar{B} \to X_s\gamma$ matrix elements using interpolation in m_c*, Nucl. Phys. B **764** (2007) 62.

[37] M. Czakon, U. Haisch and M. Misiak, *Four-Loop Anomalous Dimensions for Radiative Flavour-Changing Decays*, JHEP **03** (2007) 008.

[38] A. J. Buras, L. Merlo and E. Stamou, *The Impact of Flavour Changing Neutral Gauge Bosons on $\bar{B} \to X_s\gamma$*, JHEP **08** (2011) 124.

[39] A. Alberti, P. Gambino, K. J. Healey and S. Nandi, *Precision Determination of the Cabibbo-Kobayashi-Maskawa Element V_{cb}*, Phys. Rev. Lett. **114** (2015) 061802.

[40] M. Czakon, P. Fiedler, T. Huber, M. Misiak, T. Schutzmeier and M. Steinhauser, *The $(Q_7, Q_{1,2})$ contribution to $\overline{B} \to X_s\gamma$ at $\mathcal{O}\left(\alpha_s^2\right)$*, JHEP **04** (2015) 168.

[41] UTFIT Collaboration, "Fit results: summer 2018 at `http://www.utfit.org/UTfit/ResultsSummer2018SM`."